

Chapter 1

Standard Problems in Micromagnetics

Donald Porter and Michael Donahue

*National Institute of Standards and Technology,
100 Bureau Drive, Stop 8910, Gaithersburg, MD 20899-8910, USA
donald.porter@nist.gov*

Micromagnetics is a continuum model of magnetization processes at the nanometer scale. It is largely a computational science, and as such it faces the same issues of clarity, confidence and reproducibility as any computational effort. A curated collection of well-defined reference problems, accepted by and solved by the associated research community, can address these issues by aiding communication and identifying model shortcomings and computational obstacles. This chapter reports on one such collection, called the μ MAG Standard Problems, used by the micromagnetic research community. The collection examines hysteresis, scaling across length scales, detailed computation of magnetic energies, magnetodynamic trajectories, and spin momentum transfer. Each reference problem has proven useful in improving the micromagnetics state of the art. Recommendations distilled from this experience are presented.

1. Introduction

The design and function of many modern devices rely on an understanding of patterns of magnetization in magnetic materials at the scale of nanometers. Examples include recording heads, field sensors, spin torque oscillators, and nonvolatile magnetic memory (MRAM). To study such systems researchers employ micromagnetic models, which are continuum models of magnetic materials and magnetization processes at this scale. These models are encoded in software, and simulations compute predictions of magnetic behavior used both to design devices and to interpret measurements at the nanoscale.

For many years now there has been a discussion of how to characterize the increasing role of computation in the pursuit of scientific discovery. Notably a 2005 report¹ from the U.S. Presidential Information Technology Advisory Committee announced that “computational science now constitutes the ‘third pillar’ of scientific inquiry,” taking a position alongside theory and experiment as key components of science. While the vital importance of computation in science cannot be denied, this proposition was criticized as a claim taken too far. A strongly opposing statement

was the observation that “computation... does not yet deserve elevation to third-branch status because current computational science practice doesn’t generate routinely verifiable knowledge.”² The key criticism is that a large amount of published knowledge in the peer-reviewed literature has not included sufficient information to reproduce the computations that generated it. To be fair, the PITAC report itself took note of these and other shortcomings and included recommendations aimed at making improvements. While the deductive and empirical foundations of science have well-established practices developed over long periods of time, the expectations about the best ways to carry out and publish computational results are still taking shape. We are still far from the day where every researcher is as well-versed in verification of a computation as in calibration of an instrument, but as we continue in a world where all science now includes some element of programming, that is the goal we must pursue.

Ever since the significant growth in the reach and capacity of the Internet in the 1990s suggested feasible solutions to the problem of large-scale sharing of data and programs, there have been parties making note of the shortcomings in the publication of computational results and calling for new habits and standards to address them. A prominent example is the WaveLab collection of MATLAB routines³ implementing wavelet analysis algorithms underlying contemporary research. While these researchers have published their findings in wavelet analysis, they have also written on the importance of the reproducibility of their work. In support of these aims they have published the tools underlying their findings as well, including the software and datasets. By the power of example, the advantages of tool re-use, and the viral effect of collaborations, the WaveLab library has grown to a place of prominence in its field of study.

Over the same period of time, the practices of software development itself have developed in parallel so as to better support digital sharing and reproducibility. We have reached the point where most people employed in the practice of software development have a familiarity with toolsets explicitly designed to distribute development efforts on a global scale with a high degree of openness and freedom to extend and revise. The task still underway is the effort to bring the lessons and tools of the software engineers into the hands of scientists in ways that can be used effectively without undue burden. Efforts such as the Software Carpentry project⁴ play a key role in finding the path that delivers the greatest benefits available at a burden researchers are willing to bear.

The same trends in increasing connectivity and computational power at reasonable costs that drive the ability to compute and share results have also driven increases in expectations. More and more publications and institutions are establishing policies meant to incent and even require the sort of sharing needed to support reproducibility. Large scale projects like the Materials Genome Initiative (MGI) seek to harness the increasing capabilities to achieve the bold goal of cutting in half the time required to discover, develop and deploy new materials useful

in commercial products. MGI's Strategic Plan⁵ includes as one of four key challenges the aim of "making digital data accessible." Achieving this aim will involve establishing habits, practices and tools for effective distribution of the artifacts of reproducible computation.

This chapter examines one way the field of micromagnetic modeling has addressed questions of confidence and reproducibility by the definition of standard problems, and the collection and distribution of contributed solutions to them. Many problems of interest in micromagnetics demand computations on a large scale, where custom and research-level algorithms and implementations are necessary. The computational playing field is not fully settled and researchers benefit from significant freedom in the choice of data structures, algorithms, hardware and other details of implementation. Establishing the confidence and trust of reproducible computation in such an unstructured environment requires methods that accommodate that level of flexibility. The standard problem approach reviewed here has been suitable in service of those ends.

2. Micromagnetics

Micromagnetics is the use of computation to determine the spatial distribution of magnetization in magnetic materials as determined by the environment and the nature of the materials.

2.1. Equations of Magnetodynamics

Magnetization is conceived as a vector field \mathbf{M} , where the magnitude at each point in space is fixed while the direction may vary. The starting point of micromagnetics is the Landau-Lifshitz-Gilbert (LLG) equation^{6,7} that connects the changing magnetization direction at any point to a magnetic field \mathbf{H} at that point and a set of material parameters describing the material at that point,

$$\frac{d\mathbf{M}}{dt} = -|\gamma| \mathbf{M} \times \mathbf{H} + \frac{\alpha}{|\mathbf{M}|} \left(\mathbf{M} \times \frac{d\mathbf{M}}{dt} \right). \quad (1)$$

When expressed in SI units, both the magnetization \mathbf{M} and the magnetic field \mathbf{H} are quantities measured in amperes per meter (A/m). The first term on the right hand side of the LLG equation describes the precession of \mathbf{M} about \mathbf{H} . The gyromagnetic ratio γ is typically given the value

$$|\gamma| = 2.21 \times 10^5 \frac{\text{m}}{\text{A s}} \quad (2)$$

so that the frequency of precession agrees with the precession of a free electron spin in the presence of the same magnetic field. There is some ambiguity in the published literature concerning the sign of γ ; we insert the absolute value into LLG to be clear. The second LLG term is a phenomenological term introduced to account for energy loss in the system. It describes a damping or friction operating against the rotation

of the magnetization, characterized by the value of a dimensionless, positive value, α .

The total energy of the system, W , measured in joules, is the integral over the volume of interest of the pointwise energy density E (in J/m^3)

$$W = \int_V E(\mathbf{r}) d^3\mathbf{r}. \quad (3)$$

The energy density E is a function of the magnetization \mathbf{M} and the position \mathbf{r} , and the total energy $W = W[\mathbf{M}]$ is a functional of the magnetization \mathbf{M} . We define the effective magnetic field \mathbf{H} as the variational (or functional) derivative of the total energy,

$$\mathbf{H} = -\frac{1}{\mu_0} \frac{\delta W}{\delta \mathbf{M}} \quad (4)$$

where μ_0 is the SI permeability of free space,

$$\mu_0 = 4\pi \times 10^{-7} \frac{\text{J}}{\text{A}^2 \text{m}}. \quad (5)$$

The variational derivative can be defined component-wise as

$$\left. \frac{\delta W}{\delta M_i} \right|_{\mathbf{r}_0} = -\mu_0 H_i(\mathbf{r}_0) = \lim_{u \rightarrow 0} \frac{W[\mathbf{M} + u\mathbf{e}_i]}{\int_V |u(\mathbf{r})| d^3\mathbf{r}} \quad (6)$$

where M_i denotes the i -th component of \mathbf{M} , \mathbf{e}_i is the unit vector in the i -th coordinate direction, and $u = u(\mathbf{r})$ is a smooth function that is zero outside of a neighborhood of \mathbf{r}_0 . The limit is taken such that both $\max(|u|)$ and the support of u (and hence $\int |u|$) go to zero.⁸ (The variational derivative may also be defined somewhat more generally in terms of a weak limit.⁹) The units on u are A/m , so $\int |u|$ has units A m^2 , and therefore the units on \mathbf{H} are $(\text{A}^2 \text{m}/\text{J})(\text{J}/(\text{A m}^2))$, or A/m .

Historically, the first equation for magnetodynamics was introduced by Landau-Lifshitz in 1935.⁶ Known as the Landau-Lifshitz (LL) equation, it expresses $d\mathbf{M}/dt$ as the sum of two orthogonal terms:

$$\frac{d\mathbf{M}}{dt} = -\bar{\gamma} \mathbf{M} \times \mathbf{H} + \frac{\lambda}{|\mathbf{M}|} \mathbf{M} \times \mathbf{H} \times \mathbf{M}. \quad (7)$$

The quantities \mathbf{M} and \mathbf{H} are the same as in the LLG equation. The coefficients $\bar{\gamma}$ and λ both have units of meters per ampere-second ($\text{m}/(\text{A s})$). The $\mathbf{M} \times \mathbf{H} \times \mathbf{M}$ term is sometimes written as $-\mathbf{M} \times (\mathbf{M} \times \mathbf{H})$. In this regard note that $\mathbf{M} \times (\mathbf{H} \times \mathbf{M}) = -(\mathbf{H} \times \mathbf{M}) \times \mathbf{M} = (\mathbf{M} \times \mathbf{H}) \times \mathbf{M}$, so parentheses are not needed when written as in (7).

If $\bar{\gamma}$ and λ are defined in terms of the LLG coefficients γ and α by

$$\bar{\gamma} = \frac{|\gamma|}{1 + \alpha^2} \quad (8)$$

$$\lambda = \frac{|\gamma| \alpha}{1 + \alpha^2}, \quad (9)$$

then (1) and (7) are mathematically the same equation.¹⁰ Any trajectory of \mathbf{M} that solves one also solves the other. Nevertheless, each formulation has value for

interpretation and understanding. The LLG form (1) is most commonly used to invest the equation with physical meaning, while analysis of the LL form (7) can often reveal useful information more easily. The LL form can also be easier to work with numerically because it defines $d\mathbf{M}/dt$ explicitly in terms of \mathbf{M} and \mathbf{H} .

In the LLG formulation, we can imagine the degree of damping to increase without limit, but it's clear when we transform back to the LL form that an arbitrarily large α simply leads to shrinking values for both $\bar{\gamma}$ and λ . (The maximum value for the ratio $\alpha/(1+\alpha^2)$ is $1/2$, which occurs at $\alpha = 1$.) That is, an increasingly viscous system simply grinds to a standstill. Practical scenarios include only values of α less than or equal to 1. Within those limits, the particular value of α appropriate to a calculation is a property of the material under simulation.

In either LLG or LL form, it is clear that $d\mathbf{M}/dt$ is orthogonal to \mathbf{M} . This means that the pointwise magnitude of the magnetization does not vary over time, $|\mathbf{M}(\mathbf{r}, t)| = M_s(\mathbf{r})$ for all t . This is one of the fundamental constraints in canonical micromagnetics.

For the purposes of analyzing the magnetization dynamics, the LL form is somewhat simpler than the LLG form because the two terms on the right hand side of the LL equation are not only orthogonal to \mathbf{M} but also orthogonal to each other. The $\mathbf{M} \times \mathbf{H}$ term is orthogonal to \mathbf{H} and therefore describes precession about \mathbf{H} . Moreover, if we view the energy W as a surface over the space of magnetization configurations, then by (4) we see that \mathbf{H} is aligned with the downhill (lower energy) direction on that surface. Therefore, motion perpendicular to \mathbf{H} is energy neutral. Conversely, it follows from the vector triple product identity that $\mathbf{M} \times \mathbf{H} \times \mathbf{M}/M_s^2 = \mathbf{H} - (\mathbf{M} \cdot \mathbf{H})\mathbf{M}/M_s^2$, which is the projection of \mathbf{H} onto the space orthogonal to \mathbf{M} . In other words, the damping term in the LL equation is in the direction of the component of \mathbf{H} compatible with the magnetization norm constraint, and so motion in this direction tends to align \mathbf{M} with \mathbf{H} and lowers the energy.

It is clear from the LL form that stationary configurations, where $d\mathbf{M}(\mathbf{r})/dt = \mathbf{0}$ for all \mathbf{r} , occur exactly when $\mathbf{M}(\mathbf{r}) \times \mathbf{H}(\mathbf{r}) = \mathbf{0}$ (or equivalently, $\mathbf{M}(\mathbf{r})$ is parallel to $\mathbf{H}(\mathbf{r})$) for all \mathbf{r} . In this case both terms on the right hand side of (7) are individually zero. It follows from (4) that stable stationary configurations correspond to local energy minima. Therefore, we see that terminating configurations of LLG trajectories are local minima of the energy. For many purposes the complete dynamics of the magnetization are not important, so long as these energy-minimizing magnetization states can be determined. In such cases direct energy minimization, using for example conjugate-gradient methods, can be many times faster than solving the LLG equation.

Energy minimization is at the core of the technique known as quasi-static micromagnetics. A local energy minimum is computed at one applied field held static over the minimization step. After the equilibrium configuration is found the applied field is changed slightly (stepped) and then a new energy minimizing configuration

is sought starting from the previous energy minimum. This process is repeated across the full desired range of applied field. This method is at the heart of the first two μ MAG Standard Problems. The third μ MAG Standard Problem also directly addresses the task of energy computation.

Of course, there are many instances where the full magnetization dynamics are important, in which case there is no alternative to solving the LLG equation for the time varying magnetization. The fourth and fifth μ MAG Standard Problems are of this class.

The LLG equation is the most commonly encountered representation of magnetization dynamics for micromagnetics, and it is also the most basic. Various extensions have been proposed which can more faithfully reproduce experimental observations in some circumstances. For example, the damping factor α in the LLG equation is a phenomenological term representing the simplest way to model energy loss in a dynamic magnetic system. More complex, non-isotropic and non-local models of damping are possible.^{11–13} More radically, the norm constraint $|\mathbf{M}(\mathbf{r}, t)| = M_s(\mathbf{r})$ for all t can be relaxed with the introduction of a restoring force that instead causes $|\mathbf{M}(t)|$ to only tend toward M_s . This property underpins the Landau-Lifshitz-Bloch (LLB)^{14–17} and Landau-Lifshitz-Baryakhtar (LL-*Bar*)^{18–20} equations. New physics, such as the spin-torque effect, can be introduced with the addition of the Slonczewski spin-transfer torque term (LLGS),^{21–25} which is the subject of the fifth μ MAG Standard Problem.

Each of the μ MAG Standard Problems is presented in detail in Sec. 4. To prepare for that presentation we first examine the energy components that make up a micromagnetic simulation.

2.2. Magnetic Energy Components

The LLG equation predicts the dynamics of magnetization as a function of the magnetization configuration and the total effective field \mathbf{H} . At each point in space, $\mathbf{H}(\mathbf{r})$ can be described as a sum of magnetic fields arising from different sources. The four fundamental sources in micromagnetics are the anisotropy energy, the quantum-mechanical exchange energy, the self-magnetostatic (dipole-dipole) energy, and the Zeeman energy. Some of these components depend only on material properties and the magnetization configuration \mathbf{M} . For those terms $\mathbf{H}(\mathbf{r})$ may depend on \mathbf{M} at only the point \mathbf{r} itself (e.g., anisotropy), on \mathbf{M} in a small neighborhood of \mathbf{r} (exchange), or on \mathbf{M} globally across the entire volume of the simulation (self-magnetostatic). Other components of \mathbf{H} may be independent of the magnetization configuration \mathbf{M} . These represent the influence of the environment outside of the material of interest, and are represented as applied fields (Zeeman).

2.2.1. Anisotropy Energy

One of the simpler energy source terms is the anisotropy energy. It is the tendency of electron spins to interact with the atomic structure of the material in such a way that magnetization in certain directions is favored over others. The anisotropy energy is defined to prefer favored directions with an energy penalty for moving away from the such directions. As an example, a material with a single favored direction along an axis determined by unit vector \mathbf{u} , may be represented by the energy term

$$W_K = \int_V -K \left(\frac{\mathbf{M}}{|\mathbf{M}|} \cdot \mathbf{u} \right)^2 d^3\mathbf{r}. \quad (10)$$

Such a material is said to have a uniaxial anisotropy. The anisotropy is characterized by the value of anisotropy energy density K in units of joules per cubic meter (J/m^3). The values of K and \mathbf{u} may vary spatially. If $K > 0$ then \mathbf{u} is an easy (energetically preferred) axis for the magnetization. If $K < 0$ then \mathbf{u} is a hard axis, that is, it is energetically favorable for the magnetization to lie in the plane orthogonal to \mathbf{u} (which is known as the easy plane for magnetization).

It follows from (4) that the anisotropy field corresponding to (10) is

$$\mathbf{H}_K = \frac{2K}{\mu_0 |\mathbf{M}|^2} (\mathbf{M} \cdot \mathbf{u}) \mathbf{u}. \quad (11)$$

Other anisotropies favoring multiple axes, or having higher-order dependencies, may be specified by analogous energy terms.^{26–29} In many of these cases, the crystalline structure of the material is reflected in the energy term, and it is then known as the magneto-crystalline anisotropy. As an example, cubic anisotropy can be represented by

$$W_{K,\text{cubic}} = \int_V \frac{K}{|\mathbf{M}|^4} (M_x^2 M_y^2 + M_x^2 M_z^2 + M_y^2 M_z^2) d^3\mathbf{r} \quad (12)$$

with associated field

$$\begin{aligned} \mathbf{H}_{K,\text{cubic}} = & -\frac{2K}{\mu_0 |\mathbf{M}|^4} [M_x (M_y^2 + M_z^2) \mathbf{e}_x + M_y (M_x^2 + M_z^2) \mathbf{e}_y \\ & + M_z (M_x^2 + M_y^2) \mathbf{e}_z]. \end{aligned} \quad (13)$$

2.2.2. Exchange Energy

Micromagnetics is conceived as a continuum theory. The vector fields are taken to be continuous functions of continuous space. As a physical matter, magnetization arises from the quantum mechanical exchange interaction. In ferromagnetic materials, the effect of this quantum phenomenon is to align magnetic moments of electrons with the magnetic moments of other nearby electrons. This leads to the formation of magnetic domains within magnetic materials. In continuum micromagnetics, an exchange energy term that penalizes large spatial rates of change in magnetization

configurations achieves the same end. A conventional formulation for exchange energy is

$$W_{\text{exch}} = \int_V \frac{A}{|\mathbf{M}|^2} \left(|\nabla M_x|^2 + |\nabla M_y|^2 + |\nabla M_z|^2 \right) d^3\mathbf{r}, \quad (14)$$

where A is an exchange coefficient measured in joules per meter (J/m). This can also be written as³⁰

$$W_{\text{exch}} = \int_V -\frac{A}{|\mathbf{M}|^2} \mathbf{M} \cdot \left(\frac{\partial^2 \mathbf{M}}{\partial x^2} + \frac{\partial^2 \mathbf{M}}{\partial y^2} + \frac{\partial^2 \mathbf{M}}{\partial z^2} \right) d^3\mathbf{r}. \quad (15)$$

The corresponding expression for the exchange field is

$$\mathbf{H}_{\text{exch}} = \frac{2A}{\mu_0 |\mathbf{M}|^2} \left(\frac{\partial^2 \mathbf{M}}{\partial x^2} + \frac{\partial^2 \mathbf{M}}{\partial y^2} + \frac{\partial^2 \mathbf{M}}{\partial z^2} \right) \quad (16)$$

Since these expressions are founded on spatial derivatives of the magnetization, a set of suitable boundary conditions must be defined. When the boundary of our volume of interest corresponds to the boundary separating a magnetic material from space where magnetization is zero, the natural Neumann constraint

$$\frac{\partial \mathbf{M}}{\partial \mathbf{n}} = \mathbf{0} \quad (17)$$

takes hold, while in other situations, other choices are possible.³⁰

More complex forms for the exchange interaction are sometimes used, including anisotropic variants.³¹

2.2.3. Self-Magnetostatic Energy

Any spatial pattern of magnetization gives rise to a magnetic field $\mathbf{H}_{\text{demag}}$ as determined by the simultaneous solution of the relevant Maxwell equations,

$$\nabla \cdot \mathbf{H}_{\text{demag}} = -\nabla \cdot \mathbf{M}, \quad (18)$$

$$\nabla \times \mathbf{H}_{\text{demag}} = \mathbf{0}. \quad (19)$$

The quantity $\mathbf{H}_{\text{demag}}$ is known by many names, including “self-magnetostatic field,” “dipole-dipole field,” and “demagnetizing field.” The effects of this field are at work when matters of shape anisotropy are considered. If we imagine our continuum representation of magnetization as an approximation to a collection of discrete elementary magnets, the magnetostatic field is the field required to represent the sum of the dipole-dipole interactions of the collection of magnets. For a volume of interest V bound by a closed surface S with normal vector \mathbf{n} , the magnetostatic field is computed as

$$\mathbf{H}_{\text{demag}}(\mathbf{r}) = \frac{1}{4\pi} \int_V -\nabla' \cdot \mathbf{M}(\mathbf{r}') \frac{\mathbf{r} - \mathbf{r}'}{|\mathbf{r} - \mathbf{r}'|^3} d^3\mathbf{r}' + \frac{1}{4\pi} \int_S \mathbf{n} \cdot \mathbf{M}(\mathbf{r}') \frac{\mathbf{r} - \mathbf{r}'}{|\mathbf{r} - \mathbf{r}'|^3} d^2\mathbf{r}' \quad (20)$$

The demagnetizing field at each point is seen to be a function of \mathbf{M} throughout the volume of interest. This is a field describing long-range interactions, unlike the other energies that describe interactions in a local volume. The consequence is

that the largest part of the computational burden in a micromagnetic model is the calculation of the self-magnetostatic fields and energies.

While the exchange energy favors the formation of magnetic domains (i.e., regions of generally uniform magnetization), the magnetostatic energy tends to favor anti-parallel alignments that break up domains. The task of micromagnetics is often the computation of what equilibrium arises from these competing tendencies. Given the quantity A in J/m which characterizes the exchange energy, and the saturation magnetization $M_s = |\mathbf{M}|$ in A/m characterizing the magnetostatic energy, the expression

$$l_{\text{ex}} = \sqrt{\frac{2A}{\mu_0 M_s^2}} \quad (21)$$

is a length in meters. This quantity is known as the (magnetostatic) exchange length of the material; it is typically around 5 nm for the more common magnetic materials. For magnetically soft materials (i.e., ones with small anisotropy constant K), this is the scale of spatial features found in energy minimizing magnetization configurations, and so provides a guide to the required spatial resolution of discretizations for micromagnetic simulations. For magnetically hard materials (those with large $|K|$), another distance of interest is the magnetocrystalline-exchange length, given by

$$l_{\text{ex},K} = \sqrt{\frac{A}{K}}. \quad (22)$$

Here K is in J/m³, so again this is a length in meters. Typically the simulation discretization should be chosen smaller than either exchange length; in other words, the smaller exchange length is the controlling length scale.

2.2.4. Zeeman Energy

The effect of magnetic fields arising from outside the materials in the volume of interest is represented in a term known as the Zeeman energy. Since their origin is from outside the system, they enter the computation as inputs, typically as an applied field \mathbf{H}_{app} specified by magnitude and direction within the volume of interest. The relation between the energy and field is simply

$$W_{\text{app}} = -\mu_0 \int_V \mathbf{H}_{\text{app}} \cdot \mathbf{M} d^3\mathbf{r}. \quad (23)$$

These four energies, anisotropy, exchange, self-magnetostatic, and Zeeman, are the most commonly encountered energy sources in micromagnetic simulations. However, it is straightforward to include additional energy/field terms to represent other effects, such as thermal agitation,^{32–36} magnetoelastic behavior,^{37–39} or the Dzyaloshinskii-Moriya interaction (DMI).^{40–43}

2.3. States, Energies and Solver Requirements

The sum of the four magnetic energy terms, anisotropy, exchange, magnetostatic, and Zeeman, form the foundation of micromagnetic simulations. For many values of the parameters identifying the environmental state, and the relevant properties of the simulated materials, multiple local minima of the magnetic energy are possible. Which minimum is to be chosen is controlled by the trajectory by which it is reached, which in turn reflects the history of environmental states. This feature of the micromagnetic model provides for a representation of hysteresis in the calculation matching the hysteresis of magnetization observed in physical magnetic materials. The ability to store in the magnetic state of a material a record of the history of its environment is precisely what makes magnetic materials interesting as a building block for information storage technologies.

Magnetic materials are often characterized by their bulk properties. Given any set of parameter values characterizing material properties that govern the internal magnetic energy terms, we can find an applied field of sufficient magnitude so that the Zeeman energy term overwhelms all the others. In that extreme, in principle, only a single local minimum of magnetic energy remains, the state in which magnetization is nearly uniformly aligned with the applied field. In physical terms, we can say that we have placed the material in a state of saturation. From the saturation state, the magnitude of applied field may be reduced to zero, and then raised to a saturation value in the opposite direction and back again. In response, the bulk magnetization of the material will pass from a positive value of saturation to a negative value of saturation and back again, in a sequence of states known as the major hysteresis loop of the material. The micromagnetic model is capable of representing and computing this behavior. Key points of the major hysteresis loops are of interest in characterizing materials. The value of bulk magnetization remaining when the applied field has been reduced to zero is known as the remanent magnetization. The magnitude of reversing applied field necessary to reduce the bulk magnetization to zero is known as the coercive field, or coercivity. A validity check that a micromagnetic model properly represents a physical material is to see whether computed values of remanence and coercivity match with physical measurements.

Any software claiming to be a micromagnetic solver will have the ability to compute the energies and fields so far described, represent magnetization states, accept as inputs the material properties and initial and boundary conditions needed to describe the simulation, and output some suitable representation of the magnetization states computed as equilibrium states. The set of computations might be a numerical solution to LLG, or might be an energy-minimization approach to finding the same set of energy minima states, as appropriate to the needs of the user.

3. Obstacles to Clear Communication and Accurate Results

While there is broad common understanding in the foundations of micromagnetic modeling just described, there are also many points where variations of understanding or approach may lead to miscommunication.

The study of magnetism has a long history that has been characterized by the use of multiple systems of units. Although the SI system is becoming predominant, other systems, notably the Gaussian system, are still in use and are prevalent in historical works. This is a particular challenge because the different unit systems are not mere rescalings of one another, but the fundamental relations differ. For example, in SI we have $\mathbf{B} = \mu_0(\mathbf{M} + \mathbf{H})$, with \mathbf{B} in T and \mathbf{M} and \mathbf{H} in A/m. In the Gaussian system this renders as $\mathbf{B} = \mathbf{H} + 4\pi\mathbf{M}$ with \mathbf{H} in Oe and \mathbf{B} and $4\pi\mathbf{M}$ in G. The implication is that we not only have to contend with different sets of units, but with different equations representing the same physical phenomena. Without care, it is a common error to interact with software built on one understanding, yet select input values for it founded on a different incompatible understanding.

Another source of potential disagreement among the solutions of different micromagnetic solvers arises when the equations to be solved are mapped into representations on which to perform computations. The elements of the model equations are continuous vector and scalar fields, conceived at arbitrary precision and resolution. When we enlist computation to solve our equations, those idealized components must be reduced to one or another representation as collections of limited precision floating-point numbers held in limited stores of memory. While there are many sensible ways to do this, each brings with it limitations on the boundaries of application. The question must always be asked whether any representation, or any algorithm carried out on that representation, continues to make sense when applied to any particular problem as posed. Because different choices of representations and algorithms carry with them different limitations, it is not desirable to dictate one or another choice. It is better to let different research teams explore the differing capabilities of different choices. At the same time they must be assigned the burden of reporting the computed results in a common language that can be shared beyond the bounds of their particular assumptions.

There are sometimes also subtle issues surrounding implicit assumptions. For example, consider how one might specify the initial state of a simulation. When we speak of a part being magnetically saturated, we envision the magnetization as being uniformly oriented in the direction of an applied field. But unless the part is ellipsoidal, exactly uniform alignment is not an equilibrium state. Rather, the self-magnetostatic field will cause some canting of the magnetization near part edges and corners, as illustrated in Fig. 1. The canting will diminish as the applied field is strengthened, even to the point where it is visually difficult to distinguish between the various states, but nonetheless the differences will reemerge when the field is reduced and can influence subsequent magnetization activity. This means that specifying that a simulation begin in a saturated state is not sufficient to pin

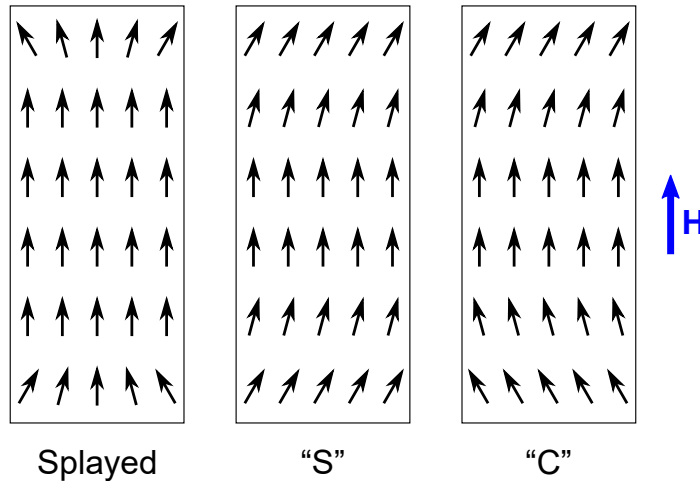


Fig. 1. Three nominally saturated magnetization states.

down subsequent behavior. Even identifying all the available equilibrium states is a non-trivial problem, a point demonstrated in Standard Problem 3.

We should point out too the difficulties posed by symmetric states, such as the “splayed” state in Fig. 1. These frequently are or devolve into saddle points on the energy surface. There are multiple, equally-valid paths forward from such states. For example, numerical round-off or other imprecisions can push the splayed state into either of the other states in Fig. 1, or their mirror images. More generally, this problem is called symmetry breaking, and must be taken into account when a simulation is being designed or described.

Identifying saddle points, which are non-stable equilibrium states, is challenging because discretization generally introduces artificial “divots” into the energy surface. That is, the discretization process can transform saddle points into shallow false minima. The size of the divots decreases as the discretization is refined, but nonetheless it is difficult to distinguish between a true shallow minimum and a false discretization-induced one.

Finally, whenever we deal with a computation performed by the execution of a computer program, we must contend with the possibility of programming error or numerical instabilities. Even with the clearest understanding of how our representations correspond to the equations we seek to solve and the physical phenomena we seek to better understand, an error in the coding of the algorithms can destroy all the value in the effort.

An ideal standard problem will take into account all of these issues. Implicit assumptions must be made explicit, so that all reported results are to the same problem. Differences in interpretations should be laid bare, so we can examine the implications of each. And for maximum impact result comparisons should help

uncover various types of programming errors.

4. A Tour of the μ MAG Standard Problems

All of these concerns about reproducible results and clear communication led to the formation of μ MAG, the Micromagnetic Modeling Activity Group in 1995. This is a loose collection of researchers, engineers, and others interested in improving the general state of micromagnetic simulation. One μ MAG activity has been the definition, publication, and sharing of solutions to a set of standard problems, intended to demonstrate proper functioning of the large collection of micromagnetic software suites. Here we examine the features and history of each standard problem.

4.1. Standard Problem 1: Hysteresis

The aim of micromagnetic modeling is to make predictions about the behavior of physical magnetic materials. It is important to establish that computed quantities have a correspondence to physical measurements. One common measurement taken on magnetic materials is the major hysteresis loop and the quantities that describe its key points. When quantities of remanence, coercivity, saturation magnetization, and various susceptibilities computed by simulation match the values measured from a physical material, we gain confidence the computed results are physically meaningful.

The first standard problem was defined to explore the reliability of micromagnetic programs carrying out this common practice. The task was to model a thin film of material measuring 2000 nm by 1000 nm by 20 nm (Fig. 2). The material was defined to have a single easy axis of anisotropy along the long dimension. The magnetic energy terms were to be computed using the prescribed values:

$$\begin{aligned}M_s &= 8.0 \times 10^5 \text{ A/m} \\ A &= 1.3 \times 10^{-11} \text{ J/m} \\ K &= 500 \text{ J/m}^3\end{aligned}$$

Contributors of submitted solutions were asked to compute and report major hysteresis loops in the plane of the modeled thin film, nominally along the long axis and the short axis. Vector field data characterizing the remanent state of their simulations was also requested, as well as descriptions of key features of the modeling and representation choices embedded in the solvers.

The specification of the first μ MAG standard problem requested anonymous submission of all contributed solutions. The aim was to encourage the submission of disappointing results as well as encouraging results, so that a complete “warts and all” picture of the state of software being used to produce published results could be sampled. Another aim was to avoid any dynamic of “proof by reputation” to take hold when it came to making judgments about which results should be trusted over others.

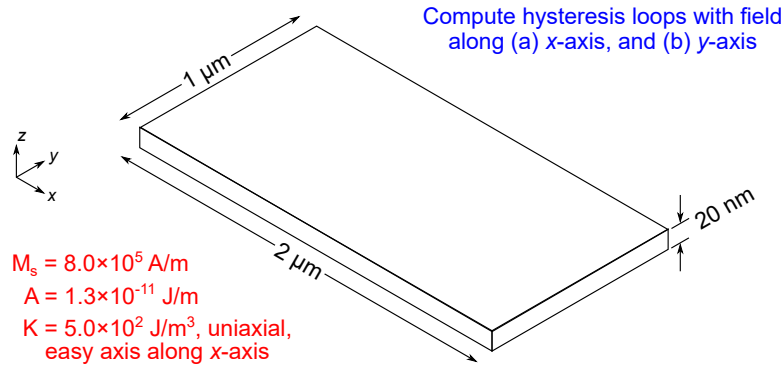


Fig. 2. Specifications for Standard Problem 1. This quasi-static problem involves anisotropy, exchange, self-magnetostatic, and Zeeman energies.

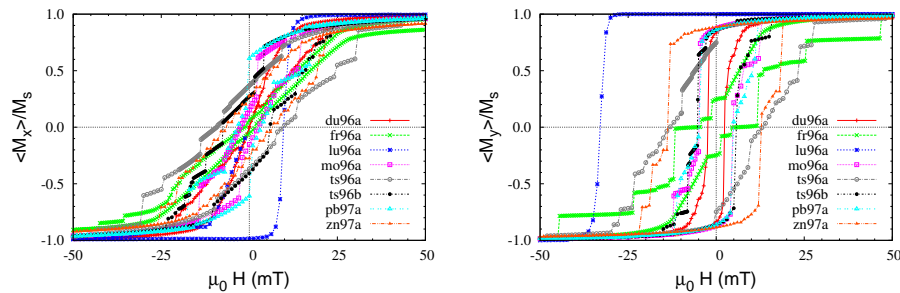


Fig. 3. Results for the eight submitted solutions to Standard Problem 1. The graph on the left shows hysteresis loops of normalized, spatially averaged M_x for field applied along the long x -axis of the sample; the right shows averaged M_y for field applied along the shorter y -axis.

Eight solutions were submitted, and the results were widely divergent. (Fig. 3). Coercivity values differed by over an order of magnitude. Some vector field submissions clearly presented non-physical results, indicating model failure, but even among the submissions with plausible appearance, the variability of key computed results was wide. The clear lesson was that published computations from micromagnetic modeling needed additional evidence of correctness to be fully trustworthy.

Examination of the submitted solutions reached the conclusion that many suffered from failures of representation (Table 1). From the specified material parameters, the exchange length is $l_{\text{ex}} = 5.7 \text{ nm}$. This suggests a resolution into computational cells with dimension of about 5 nm, or 320 000 cells for a proper representation. Not one submission had so many cells. The largest number of cells in a contributed solution was 28 026, while the smallest attempted to represent the material with a mere 800 cells.

This first standard problem was based on discussions between Tom Koehler (IBM Almaden) and Bob McMichael (NIST), following the first μMAG workshop in 1995 in San Antonio, Texas. The intent was to design a problem relevant to

Table 1. Standard Problem 1 submission details

Submission Code	Grid Type	Cell Count/ Dimensions (nm)	$\mu_0 H_c$ (mT)	
			x -axis	y -axis
du96a	2D hex	814	2.4	0.1
	2D spins	$62 \times 54 \times 20$		
fr96a	2D square	800	7.8	1.5
	2D spins	$50 \times 50 \times 20$		
lu96a	2D square	1800	32.9	9.8
	3D spins	$33 \times 33 \times 20$		
mo96a	2D square	5000	4.9	2.5
	3D spins	$20 \times 20 \times 20$		
ts96a	Irreg tetra	3353	13.0	9.3
	3D spins	$103 \times 103 \times 8$		
ts96b	Irreg tetra	2878	5.3	7.5
	3D spins	$66 \times 67 \times 20$		
pb97a	2D square	5000	4.9	3.4
	2D spins	$20 \times 20 \times 20$		
zn97a	Irreg tetra	28026	13.8	6.6
	3D spins	$30 \times 31 \times 6$		

the then-current efforts at modeling the behavior of read sensors in contemporary computer hard drives. It was not appreciated at the time, however, that the magnetization reversal inherent in Standard Problem 1 made for a significantly more challenging problem than the small-signal behavior being studied at that time. It should also be noted that the meager cell counts of the submitted solutions reflect the computational limitations of that era; twenty years later it is now commonplace to run fully 3D simulations comprising many millions of cells.

The computational limitations of that time prompted a number of simplifying assumptions. For example, models of thin films typically supposed that there was no need to represent magnetization variation through the thickness, so a single two-dimensional layer of cells was sufficient. This assumption was often made even when the material thickness measured multiple exchange lengths. Another common thin film approximation was to presume that the large shape anisotropy of the film would force all magnetization vectors into the plane of the film. This would be coded as a hard assumption that the out-of-plane component of magnetization was always zero. The language of the day spoke of “2D grids” for the former and “2D spins” for the latter. The appeal of these assumptions is clear. They greatly reduce the dimension of the problem, which in turn greatly reduces that volume of data that must be stored and processed. Software always compromises to the capabilities of hardware available at the time, but one must take care to not simplify away the physics fundamental to the problem.

Several lessons can be drawn from the experience of μ MAG Standard Problem 1. For consumers of micromagnetic simulation results, the lesson is that skepticism is

justified, and they should expect publishers of such calculations to include evidence as to why their results can be trusted. For the developers of micromagnetic solver software, the importance of representation limits was highlighted. The utility of examining the difference of magnetizations in neighboring cells was confirmed as a figure of merit. For those who aim to define standard problems, the key lesson was the importance of choosing problems at the proper scale for the broad capabilities among the submitters.

Some social lessons were learned as well. The amount of effort to contribute a solution to a standard problem must be scaled appropriately. This is especially so when an anonymous contribution is requested, as a researcher cannot expend a large fraction of resources on a task for which they can not claim credit. Subsequent standard problems have not had anonymous contributions. Instead, we expect standard problem solutions to appear as a small part of a larger article published in the regular literature. For example, oftentimes a standard problem result is included in an article as evidence of the soundness of the calculations. These considerations imply a suitable scale for being able to report results, and a suitable scale of resource expenditure. These are constraints that must be taken into account during standard problem design.

Some further design issues that were not fully appreciated until after the Standard Problem 1 results were digested were alluded to in Sec. 3. The initial state was not specified, and symmetry breaking was not explicitly called out, including in particular symmetry normal to the plane of the film. But an additional observation is that it can be difficult to determine what has gone wrong when solutions diverge. So it is a good idea when designing standard problems to try to build in support for diagnosing such circumstances.

For additional details on any of the standard problems, visit the μ MAG website.⁴⁴

4.2. *Standard Problem 2: Scaling*

In 1998 Tom Koehler, then retired, along with H. Neal Bertram, Alfred Liu, and Chris Seberino from the Center for Magnetic Recording Research, University of California at San Diego, proposed a new standard problem. The results of μ MAG Standard Problem 1 had exposed the importance of scaling a problem to be solved with the capabilities of the solvers making the calculation, and this new problem, μ MAG Standard Problem 2, was devised to address this issue in a systematic way. Rather than define a single simulation to perform, a parameterized family of simulations was defined and submitters were invited to contribute solutions over the parameter range suitable for the capabilities of their software. The overlapping parameter range of all contributed solutions could then be used as an arena of comparison. Also, if there was a parameter range where solutions agree, then the details of how the solutions diverged at the boundaries of the agreement range would help in understanding the causes of the divergence.

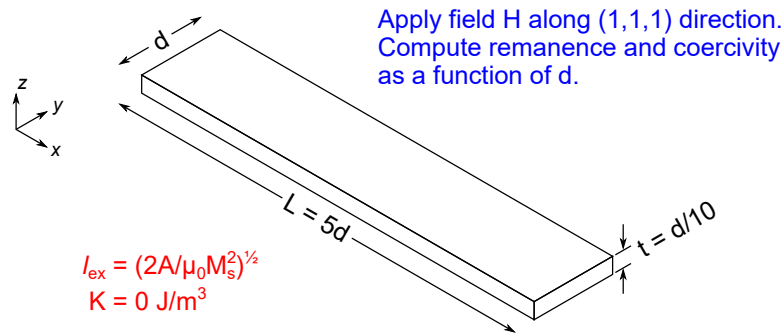


Fig. 4. Specifications for Standard Problem 2. This quasi-static problem studies the effect of part scaling on the interactions between exchange, self-magnetostatic, and Zeeman energies.

Anisotropy energy is omitted in μMAG Standard Problem 2. In other words,

$$K = 0 \text{ J/m}^3. \quad (24)$$

The values of M and A are left unspecified. Values best suited to the functioning of any contributing solver could be selected. Once values were selected, though, the corresponding exchange length, l_{ex} , defines the scale of the sample.

The simulation sample was to be a rectangular prism of magnetic material. The prism was to be $5d$ units long, d units wide, and $d/10$ units thick (see Fig. 4). The parameter d , measured in units of l_{ex} , controls the scale of the particular simulation. To illustrate, when $d = 1$, the prism is one exchange length wide, five exchange lengths long, and one tenth an exchange length thick. The large ratio of width to thickness was intended to increase the range for which solvers built on inherently 2D grids could be expected to have their constraints met.

Each contributor was free to choose key features of how magnetization patterns of the prism were to be represented. The number and type of computation cells were unspecified. However, each contributor was expected to have assured themselves that the solutions they contributed would not significantly differ with finer resolution of representation. As larger and larger values of d were considered, the expected resource consumption of a suitable computation would increase, and the contributor would choose the limit they could reach.

Having defined the geometry and material parameters, the simulated measurement to perform was once again a major hysteresis loop as in the first standard problem. This time the axis of the applied field was specified as the $[1, 1, 1]$ axis so as to avoid any difficulties that arise near axes of symmetry. Contributed solutions would identify the values of (d/l_{ex}) and the corresponding values of remanence and coercivity. The stated assumption in the problem definition was that for small values like $(d/l_{\text{ex}}) = 0.1$, the exchange energy would dominate, forcing uniform magnetization. This scenario could be well-represented with a single-spin model, relieving any burden of representation. Solution of a single-spin energy minimization problem could in principle produce the correct result, so we assumed that all

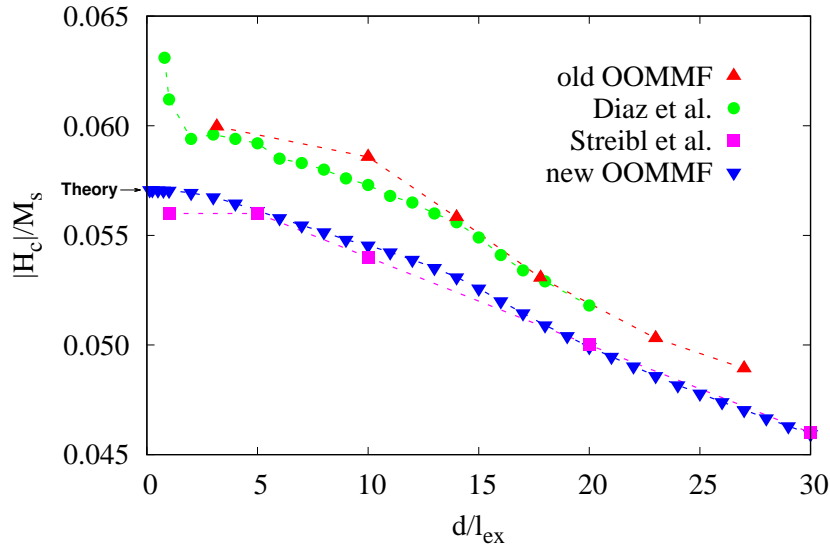


Fig. 5. Reported coercivity values for Standard Problem 2. The location marked “Theory” is the theoretical value for an infinitely small part.

minimally competent micromagnetic solvers would agree on the result at the small end of the parameter range. The expectation was that as (d/l_{ex}) grew larger the solutions would diverge, and examining the differences would help us learn how different modeling and programming choices affected simulation results.

Three solutions were published and contributed (the old OOMMF, Diaz, and Streibl curves in Fig. 5).^{45–48} The results were much more tightly clustered together than those of the first Standard Problem, and none of them included results that were clearly nonphysical. The differences in the contributed coercivity values, for example, were within a range of about 5%. Two of the solutions were in very tight agreement (old OOMMF and Diaz), while the third (Streibl) reported coercivity values about 5% smaller. All three solutions used a single layer of computational cells to represent the magnetization, and all used representations at resolutions believed suitable for the features expected in the magnetization patterns.

Most remarkable was the failure to have the expected agreement for small values of (d/l_{ex}) . One contributed solution did not even compute solutions for $(d/l_{\text{ex}}) < 3$. The other two both reported computational difficulties arising with such simulations. As the exchange energy grew to dominate the calculations, the micromagnetic solvers encountered stiffness in the calculations. Progress toward convergence became slow, and convergence with increasing spatial resolution could not be demonstrated. The simple case that all solvers were expected to agree upon was in fact not so simple.

In order to examine more carefully the particular causes of the failure of the solutions to agree, a simplified form of the problem was examined in detail.⁴⁹ When

the exchange energy dominates to the extent that a uniform magnetization is the only possible state, a single spin model can be analyzed.⁵⁰ An energy minimization analysis of a single spin can produce the remanence and coercivity values expected in the limit as $(d/l_{\text{ex}}) \rightarrow 0$. In Fig. 5, the coercivity value determined by analysis of the single spin model is marked with the label “Theory”. This value agreed best with the results of the lone solution (Streibl) among the three contributed solutions. Even more important than determining which solution was more nearly correct, the analytical results provided a target with which to examine where the other solutions had gone wrong.

The analytical computation of coercivity is achieved via a balancing of Zeeman energy and magnetostatic energy. (Exchange energy does not contribute to the solution of a single spin simulation.) Attention is focused on how micromagnetic solvers compute these quantities to determine why their results differ. In the single-spin scenario, both applied field and magnetization are uniform. The Zeeman energy calculation is clear, simple and correct. Only the magnetostatic energy is complex enough to get something wrong. The total self-magnetostatic energy is defined as

$$W_{\text{demag}} = -\frac{\mu_0}{2} \int_V \mathbf{H}_{\text{demag}} \cdot \mathbf{M} d^3\mathbf{r}, \quad (25)$$

where $\mathbf{H}_{\text{demag}}$ is computed using (20). For a discretized representation of the magnetization as a collection of uniformly magnetized cells, the approximation used for the calculation is

$$W_{\text{demag}} \approx -\frac{\mu_0}{2} \sum_k \mathbf{H}_{\text{demag},k} \cdot \mathbf{M}_k V_k, \quad (26)$$

where $\mathbf{H}_{\text{demag},k}$ and \mathbf{M}_k are the values of $\mathbf{H}_{\text{demag}}$ and \mathbf{M} at the centroid of cell k , and V_k is the cell volume of cell k . This is a common discretized approach to computing an integral, and it works well when the cell resolution is fine enough to represent the integrand. This was the method employed by the old OOMMF and the Diaz submissions; the Streibl code used an entirely different approach to compute $\mathbf{H}_{\text{demag}}$. Examination reveals, though, that while Standard Problem 2 has been scaled to represent the magnetization \mathbf{M} well, the spatial features of $\mathbf{H}_{\text{demag}}$ are not captured well enough to avoid error. A finer resolution of computation could improve this, but only if the discretization extends through the sample thickness, i.e., a 3D discretization.

However, the computational cost of a 3D discretization is not needed in this case, because instead one can revise the calculation used to approximate the integral. Because we assume magnetization is uniform within each cell, we can compute a correct per-cell energy by replacing a sample of the magnetostatic field with the average value of the magnetostatic field over the volume of the cell.

$$W_{\text{demag}} = -\frac{\mu_0}{2} \sum_k \langle \mathbf{H}_{\text{demag}} \rangle_k \cdot \mathbf{M}_k V_k. \quad (27)$$

A revised simulation based on this change does indeed agree with the analytical solution (“new OOMMF” in Fig. 5). This change also removed the stiffness and

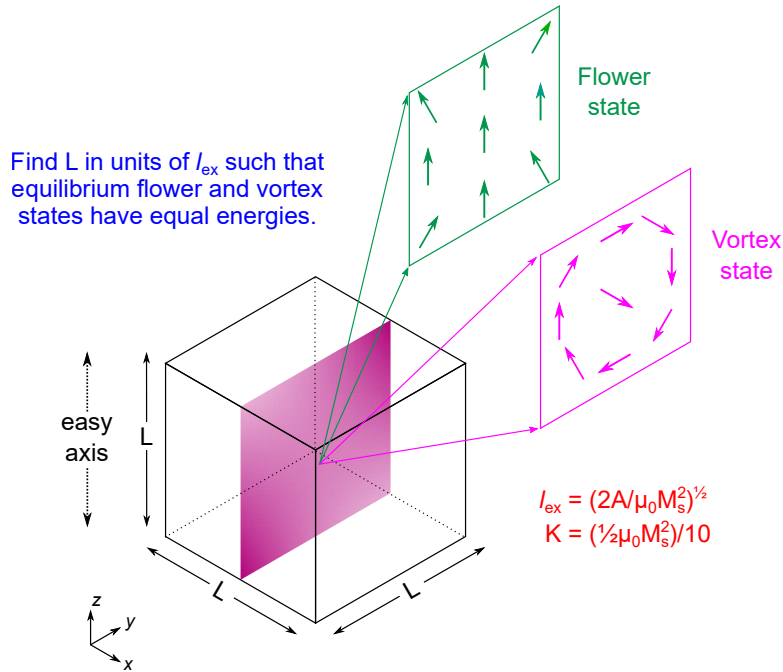


Fig. 6. Specifications for Standard Problem 3. This wholly static, direct energy minimization problem studies the balance between anisotropy, exchange, and self-magnetostatic energies.

convergence issues observed previously. This is a powerful example of a standard problem success. Although contributors worked with solvers founded on different models and techniques, their solutions could be meaningfully compared. Working through the details of disagreement on a standard problem result led to an improved code and the correction of significant error that would have been difficult to detect otherwise.

4.3. Standard Problem 3: Three Dimensional Energy Minimization

For the third standard problem, an expanded capability was demanded from solvers. The problem is defined to consider the magnetization state of a material with three significant dimensions. Any solver built on the inherent constraints and approximations of a 2D grid could not attempt this problem. This problem was proposed by Alex Hubert of the University of Erlangen-Nürnberg in 1998.

Like the second standard problem, a scaling parameter was employed. The values of M_s and A were left unspecified, but instead the corresponding exchange length, l_{ex} , was used to define the scale. A cube of edge length L , measured relative to l_{ex} , was to be simulated. A small anisotropy energy was also included to provide a definite direction to the expected solution states. The easy axis of anisotropy was aligned with the z -coordinate axis of the cube (Fig. 6). The magnitude of the

Table 2. Standard Problem 3 solution component energies

Submitter	L/l_{ex}	e_{total}	Single Domain			Vortex		
			e_{demag}	e_{exch}	e_{anis}	e_{demag}	e_{exch}	e_{anis}
Rave	8.47	.3027	.2794	.0177	.0056	.0783	.1723	.0521
Martins	8.4687	.3026	.2792	.0177	.0056	.0780	.1724	.0521
Hertel	8.57	.3032	.2332	.0466	.0233	.0821	.1689	.0521

anisotropy energy is defined relative to the saturation magnetization,

$$K = 0.05\mu_0 M_s^2. \quad (28)$$

The computed energy densities, e_* , were to be reported using the quantity

$$K_m = 0.5\mu_0 M_s^2 \quad (29)$$

as the scale of measure. On this scale, for example, the anisotropy energy e_{anis} could range from 0 to 0.1.

When (L/l_{ex}) is small enough, an energy minimizing configuration could only be a (nearly) uniform magnetization, due to domination of the exchange energy. As (L/l_{ex}) grows larger there remains only one energy minimizing configuration, though the rising influence of the magnetostatic energy pulls it away from uniformity, with a symmetric splay near the head and tail surfaces of the cube. This appearance of opening up like a flower inspires the label of a “flower” state, still essentially a single domain configuration. In this configuration there is rotational symmetry about the easy axis through the center of the cube. As (L/l_{ex}) grows larger still, it was expected that at some point the magnetostatic energy advantage of the magnetization configuration closing upon itself in a vortex formation would become important enough to break apart the single domain pattern. In this state the central core region orients along the x -axis direction, while the magnetization outside the core circulates around the core in the yz -plane. (There are also exactly equivalent symmetric solutions with the vortex core pointing in the $-x$ or $\pm y$ -axis directions.) The challenge of the problem was to find the size (L/l_{ex}) for which the total energy density of the flower state was the same as the total energy density of the vortex state.

Three solutions were contributed (Table 2). The first two were in tight agreement that a value of $(L/l_{\text{ex}}) = 8.47$ produced equal energies for the flower and vortex states.⁵¹ The third contribution reported that flower and vortex states had equal energies when $(L/l_{\text{ex}}) = 8.52$. However, the third contribution also reported the discovery of a third stable configuration.⁵² The unexpected configuration was similar to the flower state but with a helical twist along the z -axis. The contributors named this the “twisted flower” state. At simulated sizes near the solution point, the energy of the twisted flower state was less than that of the ordinary flower state. The consequence is that the size at which the energy of the vortex state matches the energy of any single-domain state is larger at $(L/l_{\text{ex}}) = 8.57$. The existence and

properties of the “twisted flower” state have been subsequently verified by other researchers. This is an example of the difficulties surrounding symmetry breaking discussed in Sec. 3.

4.4. Standard Problem 4: Dynamics

The fourth μ MAG Standard Problem was brainstormed by Bob McMichael (NIST), Roger Koch (IBM), and Thomas Schrefl (TU Wien), and developed by Jason Eicke (George Washington University) and Bob McMichael in 2000. This problem expanded the demands on contributed solutions in a different way. The prior standard problems centered around the computation of stable magnetization states. These computations could be completed entirely from a perspective of energy minimization, without an explicit need to compute full trajectories of the LLG equation. The fourth μ MAG Standard Problem explicitly calls for the reporting of those trajectories. It is the first standard problem to probe the accurate solving of the LLG equation itself. The problem dimensions are that of a thin film, however, so solution can be attempted using a 2D grid.

The material properties are an adaptation of those from the first μ MAG Standard Problem, but with anisotropy energy explicitly set to zero, and with explicit values for the dynamic parameters γ and α ,

$$A = 1.3 \times 10^{-11} \text{ J/m} \quad (30)$$

$$M = 8.0 \times 10^5 \text{ A/m} \quad (31)$$

$$K = 0 \text{ J/m}^3 \quad (32)$$

$$\gamma = 2.211 \times 10^5 \text{ m/(A s)} \quad (33)$$

$$\alpha = 0.02. \quad (34)$$

The sample to be simulated measured $500 \times 125 \times 3$ nm in the x , y , and z directions respectively (Fig. 7). To produce the initial state of the simulation, a saturating field in the $[1, 1, 1]$ direction was to be applied, and “slowly” reduced until a remanent state was reached. The precise sequence of applied fields to reach this initial state was not specified, but the initial state was prescribed to be an “S-state”, where the bulk of the sample is magnetized in a single domain along the long axis, while two end domains both have magnetization turned in the positive y direction (Fig. 8(a)). This description leaves some room for differences in the initial state of different simulations so that each simulation can begin in a state it considers to be an energy minimum within the constraints of its selection of representations and approximations.

From the initial state, two calculations of LLG trajectories are to be completed in response to two described applied fields. The first simulation calls for the instantaneous application of a uniform applied field with magnitude

$$\mu_0 |\mathbf{H}_{\text{app}}| = 25 \text{ mT} \quad (35)$$

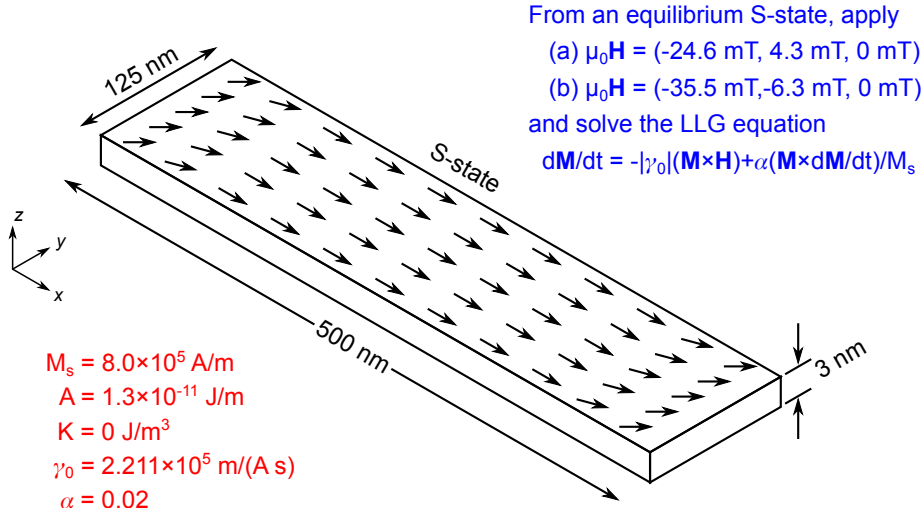


Fig. 7. Specifications for Standard Problem 4. This dynamic problem studies interactions between exchange, self-magnetostatic, and applied fields during magnetization reversal.

directed in the second quadrant of the xy -plane at an angle of 170° from the positive x axis. The magnitude is chosen to be comfortably large enough to cause a magnetization reversal, and the direction is chosen so that the reversal occurs primarily by in-plane counterclockwise rotation across the sample. The dynamics of the reversal are illustrated by the snapshots in Fig. 8. We refer to this as the “easy” reversal.

While long term behavior is determined ultimately by energy minimization considerations and hence the damping term in the LL equation ($\lambda \mathbf{M} \times \mathbf{H} \times \mathbf{M}$), for most materials the damping parameter $\lambda = |\gamma| \alpha / (1 + \alpha^2)$ is relatively small, and so over short time scales the precession term $-|\gamma| \mathbf{M} \times \mathbf{H}$ tends to dominate. That is the case here; when \mathbf{H}_{app} is first applied the magnetization precesses about the applied field and into the $-z$ direction. The darker background in Fig. 8(b) indicates this behavior. The out-of-plane movement is strongest at the ends (in the center the magnetization is nearly anti-parallel to the applied field and so the $\mathbf{M} \times \mathbf{H}$ torque is weak), but the perturbation is towards $-z$ throughout the sample. This displacement invokes a strong self-magnetostatic field in the opposite, $+z$ direction. The magnetization then precesses about the reaction field, as seen by the counterclockwise rotation evident in Fig. 8(b) and (c). The strength of the reaction field varies spatially, so the rotation is not uniform. The non-uniformity causes domain walls to form. The domain walls then collapse inward until the magnetization reversal is complete (Fig. 8(b) through (d)). After this the magnetization continues to ring down for several nanoseconds as the excess energy is damped away.

The second simulation calls for the instantaneous application of a uniform applied field with magnitude

$$\mu_0 |\mathbf{H}_{\text{app}}| = 36 \text{ mT} \quad (36)$$

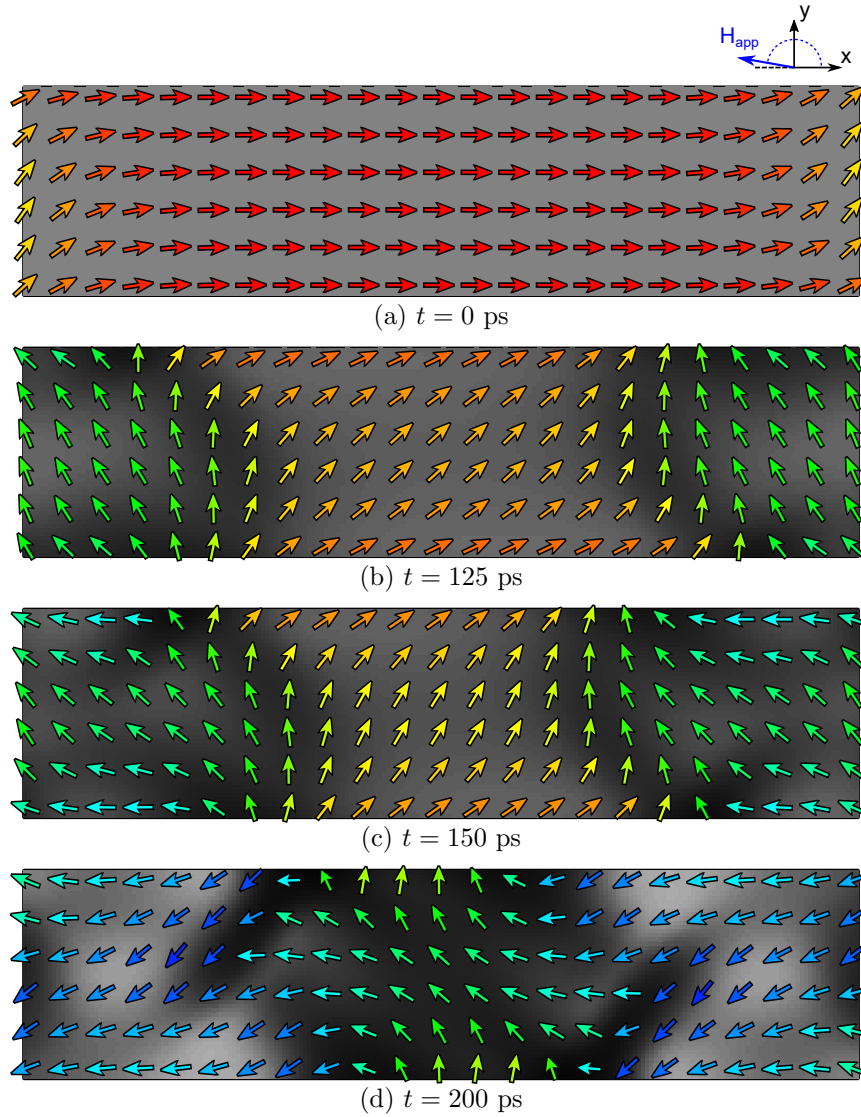


Fig. 8. Magnetization reversal Standard Problem 4 with field applied in the xy -plane at 170° from the $+x$ -axis (“easy” reversal). Dark/light background indicates magnetization is pointing into/out of the plane. Arrow color marks the in-plane angle.

directed in the xy -plane at an angle of 190° from the positive x axis (third quadrant). The mechanics of the reversal are similar to the previous one, and indeed the magnetization at the ends of the part rotate as before. But in the central part of the sample the different applied field direction causes the magnetization there to rotate upward, into the $+z$ direction. This rotation is seen in Fig. 9(a), where the light background indicates magnetization pointing upward out of the plane of

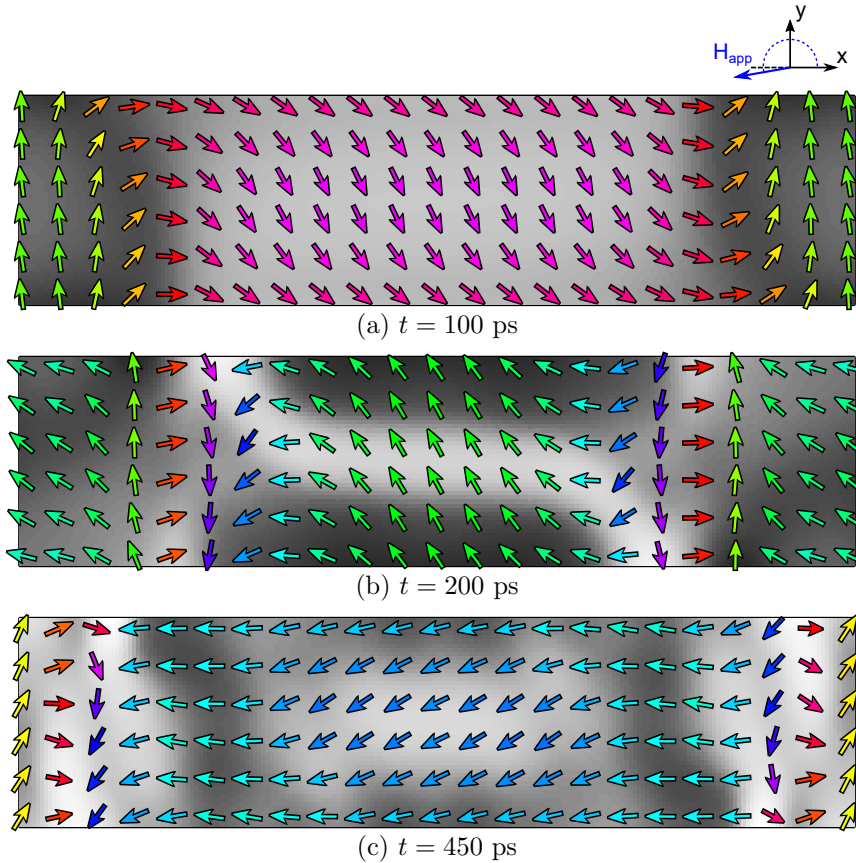


Fig. 9. Magnetization reversal Standard Problem 4 with field applied in the xy -plane at 190° from the $+x$ -axis (“complicated” reversal). The initial ($t = 0$ ps) state, shading, and color is the same as in Fig. 8. (Simulation here and in Fig. 8 performed with the OOMMF⁴⁸ package.)

the film. The component M_z produces a counter self-magnetostatic field in the $-z$ direction, and precession about this reaction field rotates the magnetization in the clockwise direction. With the magnetization at the ends rotating counterclockwise and the center rotating clockwise, by $t = 200$ ps two 360° domain walls have formed (Fig. 9(b)). As the magnetization continues to rotate these domain walls are forced outward (Fig. 9(c)) until eventually they are pushed off the ends of the part and the magnetization settles down into a new equilibrium.

The dynamics in this reversal are considerably more complex than in the preceding case. Angles between spins in adjacent computation cells are expected to grow large, challenging the approximations of representation. This “more complicated” reversal is anticipated to have greater chance of exhibiting differences among the contributed solutions.

For each simulation, contributors were asked to submit time series of the compo-

nents of spatially averaged magnetization as a characterization of the LLG trajectories. Contributions were also to include an image of the magnetization at the time when the x -component of the spatially averaged magnetization first crosses zero. The image would allow for a visual confirmation of whether different solutions had trajectories passing through visibly different intermediate states.

Nine solutions were contributed, though only a few solutions were published in conference proceedings.^{53,54} The trajectories of the “easy reversal” did indeed show close agreement among all contributions (Fig. 10 (a)). This is an important baseline result, demonstrating that when the problem is defined to avoid difficulties, many diverse solvers achieve results in agreement. It is remarkable that this is so, even though the programs in question employ a large variety of representations, models, and algorithms. The agreement among contributed solutions was less good for the “more complicated” reversal as expected (Fig. 10 (b)). Still the differences were not great, with only one significant outlier and a small amount of trajectory variation otherwise. This standard problem has become a useful tool for new micromagnetic modeling algorithms and programs to demonstrate their baseline functioning.^{55,56}

4.5. *Standard Problem 5: Spin Momentum Transfer*

The fifth μ MAG Standard Problem originated as a proposal in a published article.⁵⁷ For the first time a standard problem called for solutions of a problem requiring an extended model beyond just the LLG equation. The problem calls for an examination of the phenomenon of spin momentum transfer when an electric current flows through a magnetic material. The key observation is that electrons carry spin as well as charge. At the same time their motion creates current, that same motion moves spins through space, and those spins interact with the magnetic features of the material. The manipulation of electron spins and the interaction of those spins with patterns of magnetization form the basis of spintronics, where devices are designed to derive their functioning from these phenomena. The large and growing interest in spintronics calls for computer programs known to correctly simulate these phenomena.

The LLG equation does not contain electric currents. It must be extended to simulate spin momentum transfer. The article proposing the standard problem cites one such extension,²² expressed as the equation,

$$\begin{aligned} \frac{d\mathbf{M}}{dt} = & -\gamma \mathbf{M} \times \mathbf{H} + \frac{\alpha}{|\mathbf{M}|} \left(\mathbf{M} \times \frac{d\mathbf{M}}{dt} \right) \\ & - \frac{b}{|\mathbf{M}|^2} (\mathbf{M} \times [\mathbf{M} \times (\mathbf{J} \cdot \nabla) \mathbf{M}]) - \xi \frac{b}{|\mathbf{M}|} (\mathbf{M} \times (\mathbf{J} \cdot \nabla) \mathbf{M}). \end{aligned} \quad (37)$$

Here \mathbf{J} is the current density in amperes per square meter. The dimensionless quantity ξ represents the degree of non-adiabaticity. These two values together specify the equation to be solved. The quantity b pulls together a number of material

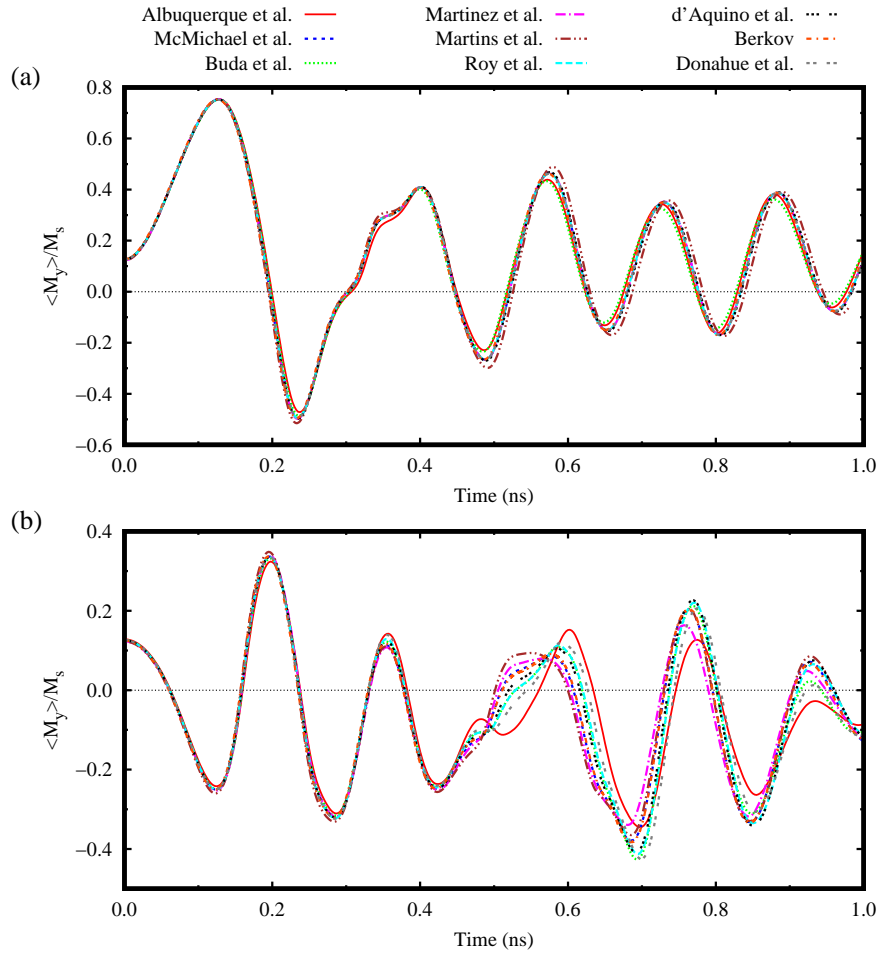


Fig. 10. Submitted results for Standard Problem 4. Part (a) shows the averaged normalized M_y value vs. simulation time for a 25 mT field applied at 170° from $+x$ -axis at time $t = 0$. Part (b) is for a 36 mT field applied at 190° from $+x$ -axis.

parameters into a value with units of cubic meters per ampere per second ($\text{m}^3/(\text{A s})$),

$$b = \frac{P\mu_B}{e|\mathbf{M}|(1 + \xi^2)}, \quad (38)$$

but it does not represent an additional independent parameter. As derived, the value b is limited to a maximum computed from the other material parameters, reaching that limit in proportion to the polarization rate of the current, P , which can be treated as a third input parameter, though one which can also be fully joined into the value of \mathbf{J} . The quantity μ_B is the Bohr magneton in joules per tesla, and the quantity e is the charge of an electron in coulombs,

$$\mu_B = 9.274 \times 10^{-24} \text{ J/T}, \quad (39)$$

$$e = 1.6022 \times 10^{-19} \text{ C}. \quad (40)$$

The proposed standard problem re-uses several parameter values from earlier problems,

$$A = 1.3 \times 10^{-11} \text{ J/m} \quad (41)$$

$$M = 8.0 \times 10^5 \text{ A/m} \quad (42)$$

$$K = 0 \text{ J/m}^3, \quad (43)$$

and the value of $\xi = 0.05$ is chosen to be sure the effects of the polarized current are clear in the simulation results. The corresponding exchange length is 5.7 nm. The current density is specified as

$$P |\mathbf{J}| = 10^{12} \text{ A/m}^2, \quad (44)$$

with the current specified to flow in the direction of the positive x axis. This specification opens the problem to solvers that do not solve the extended equation in general form, but are restricted to be able to solve only problems where electric current is uniformly in some favored direction. The material to be simulated is a thin film in the xy -plane with dimensions of $100 \text{ nm} \times 100 \text{ nm} \times 10 \text{ nm}$. A full dynamic solution is to be computed using the extended LLG equation with

$$\gamma = 2.211 \times 10^5 \text{ m/(A s)} \quad (45)$$

$$\alpha = 0.1. \quad (46)$$

An initial magnetization configuration of an in-plane vortex was specified, with a preliminary computation with $\mathbf{J} = \mathbf{0}$ performed to verify an initial state that was a stable configuration of magnetization in the sample when no current flows. Having found that initial state, the current is set to its non-zero value, and the equations are solved as simulated time passes. The position of the vortex is expected to move while the structure of the vortex remains undisturbed. The computation results to compare are the final position of the vortex, as well as data characterizing the trajectory by which the vortex reaches that position.

The article proposing this standard problem also included the computed solutions produced by four software tools available to the authors, demonstrating good agreement among them all, and attributing the minor differences to different approximations made in the calculation of magnetostatic fields and energies.

Two difficulties arose in the consideration of this proposed problem to be adopted by μMAG . First it became clear that the extension terms of the equation involve spatial derivatives of magnetization. Just as for the exchange energy calculation, matters of boundary conditions must be handled with care, and all solvers must agree on what they are in order to truly be solving the same problem. This shortcoming was easily handled by adding to the problem the constraint that the applied current must deliver zero spin torque to the magnetization at the boundary surface (i.e., the current is unpolarized at the boundary).

The second difficulty proved to be far more serious. Other developers of software to simulate spin momentum transfer had chosen to base their efforts on a formally

different extension of LLG,²³

$$\begin{aligned} \frac{d\mathbf{M}}{dt} = & -\gamma \mathbf{M} \times \mathbf{H} + \frac{\alpha}{|\mathbf{M}|} \left(\mathbf{M} \times \frac{d\mathbf{M}}{dt} \right) \\ & - (\mathbf{u} \cdot \nabla) \mathbf{M} + \frac{\beta}{|\mathbf{M}|} (\mathbf{M} \times (\mathbf{u} \cdot \nabla) \mathbf{M}). \end{aligned} \quad (47)$$

As newly discovered and measured phenomena are first represented as mathematical models, it is not uncommon for multiple formalisms to be presented until one becomes accepted. This work takes place in parallel with the development of computer models, so different programs founded on different modeling approaches are also not uncommon. When a problem to be solved is specified in the context of one equation, but it must be solved with software derived from the assumption of a different equation, the relationship between the two approaches needs to be understood at a very fine level of detail. What does it mean to set the value $\xi = 0.05$ as an input to a program that has no connection to anything named ξ ?

A careful analysis of Eq. (37) and Eq. (47) determines they represent the same equation when

$$\beta = \xi, \quad (48)$$

$$\mathbf{u} = -b\mathbf{J}. \quad (49)$$

However the derivation of Eq. (47) calls for the relationship,

$$\mathbf{u} = -\frac{gP\mu_B}{2e|\mathbf{M}|}\mathbf{J}. \quad (50)$$

The new quantity g is the dimensionless electron g -factor, and it must have the value $g = 2$ to agree with the value of γ already specified for this problem. The consequence is that the derivation of Eq. (47) demands the relationship,

$$\mathbf{u} = -b(1 + \xi^2)\mathbf{J}. \quad (51)$$

That is, the two derivations are based on different assumptions about the way the degree of non-adiabaticity ξ influences the parameters of the equation. They agree precisely only when $\xi = 0$ and disagree more and more as the value of ξ grows larger. When a solution to Eq. (37) is to be computed, and the tool at hand is software founded on the prescriptions of Eq. (47), the inputs have to adjusted to compensate for the different models incorporated in the programs. Within the usual constraints on which values are available to modify as inputs, it is most likely the adjustment will be made by scaling the value of \mathbf{J} to produce the prescribed solution. When ξ is near zero, as is most often the case in simulations of physical interest, the consequences of this detail are small, and can easily go undetected. The unit dimensions offer no clue that anything has gone wrong either.

To improve the ability of the standard problem to highlight this issue and capture any errors rooted in a mistranslation between the two formulations, μMAG Standard Problem 5 calls for four simulations to be performed for the values of $\xi = 0, 0.05, 0.1,$ and 0.5 (Fig. 11).

Two solutions have been contributed. They show good agreement with each other over all four simulations and with the other four solutions included in the original proposal on the single common simulation performed by all of them (Fig. 12).

Starting from equilibrium vortex state, apply polarized in-plane current $PJ = 10^{12}$ A/m², and solve LLGS with non-adiabaticity factor ξ set to (a) 0, (b) 0.05, (c) 0.1, and (d) 0.5.

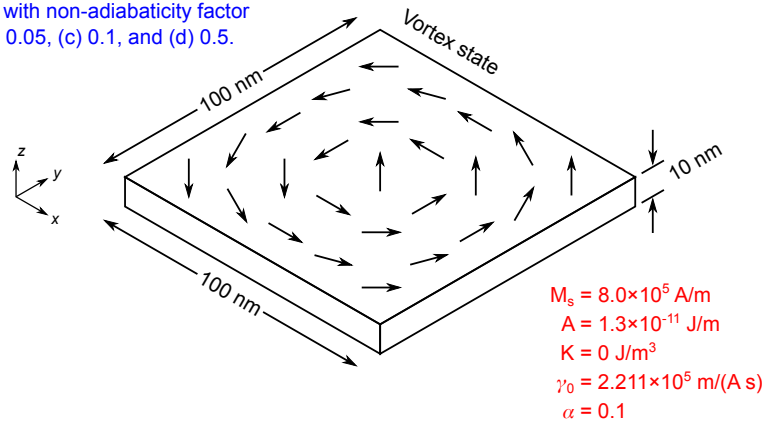


Fig. 11. Specifications for Standard Problem 5. This dynamic problem solves the Landau-Lifshitz-Gilbert-Slonczewski (LLGS) spin-torque equation with contributions from exchange and self-magnetostatic fields.

5. Conclusions

The collection of μ MAG standard problems has made positive contributions toward the aim of reliable and reproducible computation from micromagnetic modeling software. Their development has brought attention to the importance of many subtle issues in the development and use of such programs. Program errors have been located and corrected. Programs have been revised to more faithfully compute according to the assumptions of their models. Models have been carefully analyzed to determine which ones are different but equivalent formulations of the same mathematical relationships, and which ones have lurking within them true modeling disagreements. These analyses point the way to the parameter values and physical materials with the potential to select between them.

The μ MAG Standard Problems have been key in the development of best practices for effective comparisons of work from different teams employing different approaches. Some problems have exhibited the failures while others have demonstrated effective ways of addressing those same difficulties. When defining standard problems, consider these recommendations.

- A standard problem needs to be clearly stated. Write out all equations. Identify units of all quantities. Spell out any implicit assumptions like boundary conditions. Do not confuse clarity with overconstraint. Leave freedom for different approaches to solving a clearly stated problem.
- When possible, design a problem that has an analytic solution, or one that can be solved using simplified models less likely to encounter errors.
- A parameterized collection of problems is often better than a single problem. The

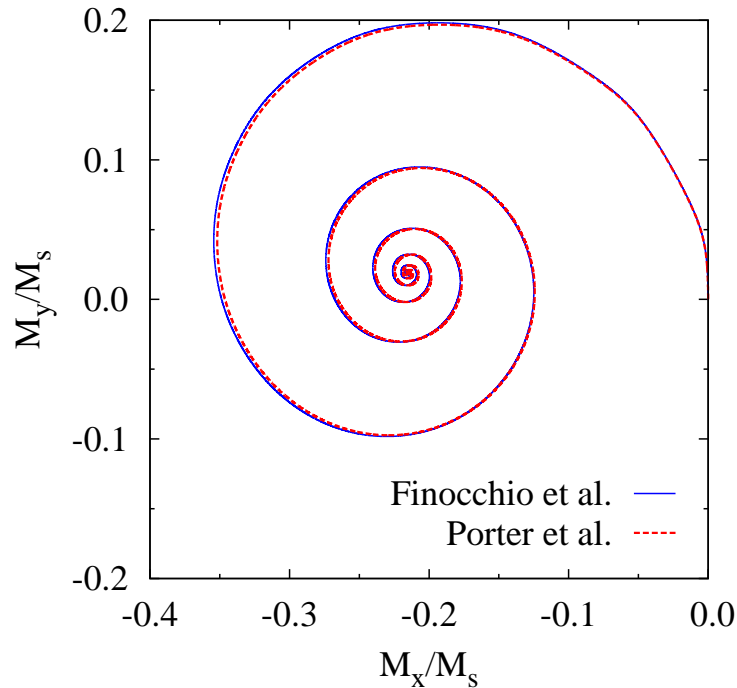


Fig. 12. Standard Problem 5 results, normalized $M_y(t)$ vs. $M_x(t)$ for $\xi = 0.05$.

differences among solutions to one problem are not as enlightening as the trends of differences among solutions to a sequence of related problems.

- Design the problem to be suitable for the known capabilities of those teams expected to submit solutions. Take care not to impose barriers that exclude submissions for reasons unrelated to the aims of the problem. Seek to discover any consequences of known different approaches. Avoid or address known confounding issues like symmetry breaking and numerical instability that are not related to the problem's purpose.
- Collect enough information in submitted solutions to not only discover differences, but to analyze the sources of those differences. Seek to establish figures of merit for establishing solution correctness.
- Design the problem to be solveable and to have its solutions submittable at an appropriate scale of effort. This includes an assessment of both computational burden and researcher effort.

The existence of the μ MAG standard problems, and the noteworthy failure of some of them to produce widespread agreement on solutions has focused attention on the need for care and judgment when reporting or relying on any computational result. Increased attention leads to more careful work, which builds greater confidence in the use of computation to establish new scientific knowledge.

Many of the problems defined and published many years ago still find use as proving grounds for new models, algorithms and implementations. It is common for researchers crafting a new program to demonstrate correctness with standard problem results, while presenting the benefits of the program in terms of increased performance, scale, or applicability to new computing hardware.^{58,59}

New standard problems will be developed as guided by the interest and participation of the μ MAG membership. Tests of more model extensions to account for newly demonstrated physical phenomena are likely, driven by both scientific and engineering interest. Published proposals already include examinations of the reliability of simulations of ferromagnetic resonance measurements⁶⁰ and spin wave dispersion.⁶¹ There is also interest in examination of the parameters that control computation, distinct from those that represent physical variations. The results computed by the conjugate gradient method of energy minimization can vary with computational choices. A carefully chosen problem⁶² brings that issue into clear focus.

Continued interest in the physics of nanomagnets and continued development of scientific computing make continued relevance and interest in micromagnetic standard problems very likely. In combination with other efforts to improve reproducibility of computation in research, confidence in the contributions of micromagnetic modeling should only improve.

References

1. M. R. Benioff and E. D. Lazowska. Computational Science: Ensuring America's Competitiveness. Technical report, President's Information Technology Advisory Committee (June, 2005).
2. D. L. Donoho, A. Maleki, I. U. Rahman, M. Shahram, and V. Stodden, Reproducible research in computational harmonic analysis, *Computing in Science & Engineering*. **11**(1), (2009).
3. J. Buckheit, J. B. Buckheit, D. L. Donoho, and D. L. Donoho. Wavelab and reproducible research. pp. 55–81. Springer-Verlag, (1995).
4. G. Wilson, D. A. Aruliah, C. T. Brown, N. P. Chue Hong, M. Davis, R. T. Guy, S. H. D. Haddock, K. D. Huff, I. M. Mitchell, M. D. Plumbley, B. Waugh, E. P. White, and P. Wilson, Best practices for scientific computing, *PLOS Biology*. **12**(1), 1–7 (01, 2014). doi: 10.1371/journal.pbio.1001745.
5. National Science and Technology Council. Materials genome initiative strategic plan. Technical report, National Science and Technology Council (December, 2014).
6. L. Landau and E. Lifshitz, On the theory of the dispersion of magnetic permeability in ferromagnetic bodies, *Physikalische Zeitschrift Der Sowjetunion*. **8**, 153–169, (1935).
7. T. L. Gilbert, A Lagrangian formulation of the gyromagnetic equation of the magnetization field, *Physical Review*. **100**(4), 1243 (November, 1955).
8. I. M. Gelfand and S. Fomin, *Calculus of Variations*, p. 29. Prentice-Hall, Englewood Cliffs, N.J., (1963).
9. R. G. Parr and W. Yang, *Density-Functional Theory of Atoms and Molecules*, pp. 246–254. Oxford University Press, New York, (1989).

10. J. C. Mallinson, On damped gyromagnetic precession, *IEEE Trans. Magn.* **23**(4), 2003–2004 (July, 1987).
11. S. Zhang and S. S.-L. Zhang, Generalization of the Landau-Lifshitz-Gilbert equation for conducting ferromagnetics, *Physical Review Letters*. **102**, 086601, (2009). doi: 10.1103/PhysRevLett.102.086601.
12. Y. Tserkovnyak, E. M. Hankiewicz, and G. Vignale, Transverse spin diffusion in ferromagnets, *Physical Review B*. **79**, 094415, (2009). doi: 10.1103/PhysRevB.79.094415.
13. W. Wang, M. Dvornik, M.-A. Bisotti, D. Chernyshenko, M. Beg, M. Albert, A. Vansteenkiste, B. V. Waeyenberge, A. N. Kuchko, V. V. Kruglyak, and H. Fangohr, Phenomenological description of the nonlocal magnetization relaxation in magnonics, spintronics, and domain-wall dynamics, *Physical Review B*. **92**, 054430, (2015). doi: 10.1103/PhysRevB.92.054430.
14. D. A. Garanin and O. Chubykalo-Fesenko, Thermal fluctuations and longitudinal relaxation of single-domain magnetic particles at elevated temperatures, *Physical Review B*. **70**, 212409, (2004). doi: 10.1103/PhysRevB.70.212409.
15. U. Atxitia and O. Chubykalo-Fesenko, Ultrafast magnetization dynamics rates within the Landau-Lifshitz-Bloch model, *Physical Review B*. **84**, 144414, (2011). doi: 10.1103/PhysRevB.84.144414.
16. R. F. L. Evans, D. Hinzke, U. Atxitia, U. Nowak, R. W. Chantrell, and O. Chubykalo-Fesenko, Stochastic form of the Landau-Lifshitz-Bloch equation, *Physical Review B*. **85**, 014433, (2012). doi: 10.1103/PhysRevB.85.014433.
17. U. Atxitia, D. Hinzke, and U. Nowak, Fundamentals and applications of the Landau-Lifshitz-Bloch equation, *J. Phys. D: Appl. Phys.* **50**(3), 033003, (2017). doi: 10.1088/1361-6463/50/3/033003.
18. V. G. Bar'yakhtar, Phenomenological description of relaxation processes in magnets, *Sov. Phys. JETP*. **60**, 863–867, (1984).
19. Y. Au, M. Dvornik, T. Davison, E. Ahmad, P. S. Keatley, A. Vansteenkiste, B. V. Waeyenberge, and V. V. Kruglyak, Direct excitation of propagating spin waves by focused ultrashort optical pulses, *Physical Review Letters*. **110**, 097201, (2013). doi: 10.1103/PhysRevLett.110.097201.
20. M. Dvornik, A. Vansteenkiste, and B. V. Waeyenberge, Thermodynamically self-consistent non-stochastic micromagnetic model for the ferromagnetic state, *Applied Physics Letters*. **105**, 162411, (2014). doi: 10.1063/1.4900428.
21. J. C. Slonczewski, Current-driven excitation of magnetic multilayers, *Journal of Magnetism and Magnetic Materials*. **159**, L1–L7 (June, 1996).
22. S. Zhang and Z. Li, Roles of nonequilibrium conduction electrons on the magnetization dynamics of ferromagnets, *Physical Review Letters*. **93**, 127204 (September, 2004).
23. A. Thiaville, Y. Nakatani, J. Miltat, and Y. Suzuki, Micromagnetic understanding of current-driven domain wall motion in patterned nanowires, *EPL (Europhysics Letters)*. **69**(6), 990–996, (2005). doi: 10.1209/epl/i2004-10452-6.
24. D. C. Ralph and M. D. Stiles, Spin transfer torques, *Journal of Magnetism and Magnetic Materials*. **320**(7), 1190–1216, (2008). doi: 10.1016/j.jmmm.2007.12.019.
25. C.-Y. You, The critical current density in composite free layer structures for spin transfer torque switching, *Journal of Applied Physics*. **107**, 073911, (2010). doi: 10.1063/1.3369582.
26. R. L. Stamps, L. Louail, M. Hehn, M. Gester, and K. Ounadjela, Anisotropies, cone states, and stripe domains in Co/Pt multilayers, *Journal of Applied Physics*. **81**, 4751–4753, (1997). doi: 10.1063/1.365452.
27. K. N. Martin, P. A. J. de Groot, B. D. Rainford, K. Wang, G. J. Bowden, J. P. Zimmermann, and H. Fangohr, Magnetic anisotropy in the cubic Laves REFe_2 inter-

- metallic compounds, *Journal of Physics: Condensed Matter*. **18**, 459–478, (2006). doi: 10.1088/0953-8984/18/2/009.
28. M. Franchin, J. P. Zimmermann, T. Fischbacher, G. Bordignon, P. A. J. de Groot, and H. Fangohr, Micromagnetic modelling of the dynamics of exchange springs in multi-layer systems, *IEEE Transactions on Magnetics*. **43**, 2887–2889, (2007). doi: 10.1109/TMAG.2007.892596.
 29. J. M. Shaw, H. T. Nembach, M. Weiler, T. J. Silva, M. Schoen, J. Z. Sun, and D. C. Worledge, Perpendicular magnetic anisotropy and easy cone state in Ta/Co₆₀Fe₂₀B₂₀/MgO, *IEEE Magnetics Letters*. **6**, 3500404, (2015). doi: 10.1109/LMAG.2015.2438773.
 30. M. J. Donahue and D. G. Porter, Exchange energy formulations for 3D micromagnetics, *Physica B: Condensed Matter*. **343**, 177–183, (2004).
 31. D. M. Schaadt, R. Engel-Herbert, and T. Hesjedal, Effects of anisotropic exchange on the micromagnetic domain structures, *Physica Status Solidi (B)*. **244**, 1271–1279, (2007). doi: 10.1002/pssb.200642613.
 32. W. F. Brown, Jr., Thermal fluctuation of fine ferromagnetic particles, *IEEE Trans. Magn.* **15**, 1196–1208, (1979).
 33. J. L. García-Palacios and F. J. Lázaro, Langevin-dynamics study of the dynamical properties of small magnetic particles, *Physical Review B*. **58**, 14937, (1998). doi: 10.1103/PhysRevB.58.14937.
 34. V. Tsiantos, W. Scholz, D. Suess, T. Schrefl, and J. Fidler, The effect of the cell size in Langevin micromagnetic simulations, *Journal of Magnetism and Magnetic Materials*. **242–245**, 999–1001, (2002). doi: 10.1016/S0304-8853(01)01365-8.
 35. E. Martínez, L. López-Díaz, L. Torres, and C. J. García-Cervera, Minimizing cell size dependence in micromagnetics simulations with thermal noise, *J. Phys. D: Appl. Phys.* **40**, 942–948, (2007). doi: 10.1088/0022-3727/40/4/003.
 36. E. Martínez, L. López-Díaz, L. Torres, C. Tristan, and O. Alejos, Thermal effects in domain wall motion: Micromagnetic simulations and analytical model, *Physical Review B*. **75**, 174409, (2007). doi: 10.1103/PhysRevB.75.174409.
 37. C.-Y. Liang, S. M. Keller, A. E. Sepulveda, A. Bur, W.-Y. Sun, K. Wetzlar, and G. P. Carman, Modeling of magnetoelastic nanostructures with a fully coupled mechanical-micromagnetic model, *Nanotechnology*. **25**, 435701, (2014). doi: 10.1088/0957-4484/25/43/43570.
 38. Y. Yahagi, B. Harteneck, S. Cabrini, and H. Schmidt, Controlling nanomagnet magnetization dynamics via magnetoelastic coupling, *Physical Review B*. **90**, 140405(R), (2014). doi: 10.1103/PhysRevB.90.140405.
 39. R. Duflou, F. Ciubotaru, A. Vaysset, M. Heyns, B. Sorée, I. P. Radu, and C. Adelman, Micromagnetic simulations of magnetoelastic spin wave excitation in scaled magnetic waveguides, *Applied Physics Letters*. **111**, 192411, (2017). doi: 10.1063/1.5001077.
 40. S. Rohart and A. Thiaville, Skyrmion confinement in ultrathin film nanostructures in the presence of Dzyaloshinskii-Moriya interaction, *Physical Review B*. **88**, 184422, (2013). doi: 10.1103/PhysRevB.88.184422.
 41. O. Boulle, S. Rohart, L. D. Buda-Prejbeanu, E. Jué, I. M. Miron, S. Pizzini, J. Vogel, G. Gaudin, and A. Thiaville, Domain wall tilting in the presence of the Dzyaloshinskii-Moriya interaction in out-of-plane magnetized magnetic nanotracks, *Physical Review Letters*. **111**, 217203, (2013). doi: 10.1103/PhysRevLett.111.217203.
 42. B. Schweglinghaus, B. Zimmermann, M. Heide, G. Bihlmayer, and S. Blügel, Role of Dzyaloshinskii-Moriya interaction for magnetism in transition-metal chains at Pt step edges, *Physical Review B*. **94**, 024403, (2016). doi: 10.1103/PhysRevB.94.024403.

43. L. Camosi, N. Rougemaille, O. Fruchart, J. Vogel, and S. Rohart, Micromagnetics of antiskyrmions in ultrathin films, *Physical Review B*. **97**, 134404, (2018). doi: 10.1103/PhysRevB.97.134404.
44. μ MAG—Micromagnetic Modeling Activity Group. <https://www.ctcms.nist.gov/~rdm/mumag.org.html>. Accessed: 2018-05-31.
45. B. Streibl, T. Schrefl, and J. Fidler, Dynamic FE simulation of μ MAG standard problem no. 2, *J. Appl. Phys.* **85**(8), 5819–5821 (April, 1999).
46. R. D. McMichael, M. J. Donahue, D. G. Porter, and J. Eicke, Comparison of magnetostatic field calculation methods on two-dimensional square grids as applied to a micromagnetic standard problem, *J. Appl. Phys.* **85**(8), 5816–5818 (April, 1999).
47. L. Lopez-Diaz, O. Alejos, L. Torres, and J. I. Igiguez, Solutions to micromagnetic standard problem no. 2 using square grids, *J. Appl. Phys.* **85**(8), 5813–5815 (April, 1999).
48. OOMMF—Object Oriented MicroMagnetic Framework. <https://www.math.nist.gov/oommf.html>. Accessed: 2018-05-31.
49. M. J. Donahue, D. G. Porter, R. D. McMichael, and J. Eicke, Behavior of μ MAG standard problem no. 2 in the small particle limit, *J. Appl. Phys.* **87**(8), 5520–5522 (April, 2000).
50. M. J. Donahue and D. G. Porter, Analysis of switching in uniformly magnetized bodies, *IEEE Trans. Magn.* **38**(5), 2468–2470 (September, 2002).
51. W. Rave, K. Fabian, and A. Hubert, Magnetic states of small cubic particles with uniaxial anisotropy, *Journal of Magnetism and Magnetic Materials*. **190**, 332–348 (Dec., 1998). doi: 10.1016/S0304-8853(98)00328-X.
52. R. Hertel and H. Kronmüller, Finite element calculations on the single-domain limit of a ferromagnetic cube—a solution to μ MAG standard problem no. 3, *Journal of Magnetism and Magnetic Materials*. **238**(2), 185–199, (2002). ISSN 0304-8853. doi: 10.1016/S0304-8853(01)00876-9.
53. R. D. McMichael, M. J. Donahue, D. G. Porter, and J. Eicke, Switching dynamics and critical behavior of standard problem no. 4, *J. Appl. Phys.* **89**, 7603–7605 (June, 2001).
54. V. D. Tsiantos, D. Suess, T. Schrefl, and J. Fidler, Stiffness analysis for the micromagnetic standard problem no. 4, *Journal of Applied Physics*. **89**(11), 7600–7602, (2001). doi: 10.1063/1.1355355.
55. M. d’Aquino, C. Serpico, and G. Miano, Geometrical integration of Landau-Lifshitz-Gilbert equation based on the mid-point rule, *Journal of Computational Physics*. **209**, 730–753, (2005).
56. C. Abert, F. Bruckner, C. Vogler, R. Windl, R. Thanhoffer, and D. Suess, A full-fledged micromagnetic code in fewer than 70 lines of numpy, *Journal of Magnetism and Magnetic Materials*. **387**, 13 – 18, (2015). ISSN 0304-8853. doi: 10.1016/j.jmmm.2015.03.081.
57. M. Najafi, B. Krüger, S. Bohlens, M. Franchin, H. Fangohr, A. Vanhaverbeke, R. Al-lenspach, M. Bolte, U. Merkt, D. Pfannkuche, D. P. F. Möller, and G. Meier, Proposal for a standard problem for micromagnetic simulations including spin-transfer torque, *Journal of Applied Physics*. 105(11):113914, (2009). doi: 10.1063/1.3126702.
58. A. Vansteenkiste, J. Leliaert, M. Dvornik, M. Helsen, F. Garcia-Sanchez, and B. V. Waeyenberge, The design and verification of mumax3, *AIP Advances*. **4**(10), 107133, (2014). doi: 10.1063/1.4899186.
59. L. Exl, J. Fischbacher, A. Kovacs, H. zelt, M. Gusenbauer, and T. Schrefl, Preconditioned nonlinear conjugate gradient method for micromagnetic energy minimization (01. 2018).

60. A. Baker, M. Beg, G. Ashton, M. Albert, D. Chernyshenko, W. Wang, S. Zhang, M.-A. Bisotti, M. Franchin, C. L. Hu, R. Stamps, T. Hesjedal, and H. Fangohr, Proposal of a micromagnetic standard problem for ferromagnetic resonance simulations, *Journal of Magnetism and Magnetic Materials*. **421**, 428 – 439, (2017). ISSN 0304-8853. doi: <https://doi.org/10.1016/j.jmmm.2016.08.009>. URL <http://www.sciencedirect.com/science/article/pii/S0304885316307545>.
61. G. Venkat, D. Kumar, M. Franchin, O. Dmytriiev, M. Mruczkiewicz, H. Fangohr, A. Barman, M. Krawczyk, and A. Prabhakar, Proposal for a standard micromagnetic problem: Spin wave dispersion in a magnonic waveguide, *IEEE Trans. Magn.* **49**(1), 524–529 (Jan, 2013).
62. J. Fischbacher, A. Kovacs, H. Oezelt, T. Schrefl, L. Exl, J. Fidler, D. Suess, N. Sakuma, M. Yano, A. Kato, T. Shoji, and A. Manabe, Nonlinear conjugate gradient methods in micromagnetics, *AIP Advances*. **7**(4), 045310, (2017). doi: 10.1063/1.4981902.